Available online at www.sciencedirect.com
SCIENCE DIRECT
Journal of Power Sources 157 (2006) 244–252
JOURNAL OF POWER SOURCES
www.elsevier.com/locate/jpowsour

Characterisation of direct methanol fuel cells under near-ambient conditions

Anders Oedegaard *

Fraunhofer Institute for Solar Energy Systems ISE, Heidenhofstr. 2, 79110 Freiburg, Germany

Received 28 February 2005; received in revised form 22 June 2005; accepted 22 June 2005
Available online 24 February 2006

Abstract

Direct methanol fuel cells have been characterised under ambient conditions. By operating the cathode with hydrogen as well as air, the half-cell and full-cell overvoltages have been found. Both the anode and the cathode kinetics improve with increasing temperature, but the cathode suffers from additional losses due to methanol crossover and water flooding. The methanol concentration, however, mainly influences the cathode. Impedance spectroscopy measurements on single cells and stacks confirm these results, and indicate that water removal from the cathode is important for stable operation of direct methanol fuel cells. Carbon dioxide (CO_2) in the cathode outlet was measured by mass spectroscopy (MS). The amount of carbon dioxide crossover is noticeable compared to the methanol crossover, but decreases with temperature and methanol concentration. Almost 100% of the crossover methanol is converted to carbon dioxide at the cathode.

Keywords: DMFC; Ambient conditions; Characterisation; Impedance spectroscopy; Mass spectroscopy

1. Introduction

Direct methanol fuel cells (DMFC) are increasingly being developed to replace or support batteries in portable applications. This is principally due to the high energy density of methanol (MeOH), which is also already available for potential consumers. Other advantages are the convenience of operating with a liquid fuel and the overall simple system design, as the complex humidification and thermal management associated with the polymer electrolyte membrane fuel cell (PEMFC) can be avoided [1].

The performance of the direct methanol fuel cell is primarily limited by the crossover of methanol and the slow kinetics of the redox reactions [2]. Both the oxidation of methanol and the reduction of oxygen leads to large overpotentials on the anode and cathode, respectively. In order to improve the activity at the electrodes, it is necessary to understand the reaction mechanism. Although various parallel reaction paths for the methanol oxidation are possible, there is consensus about the general course of action [1,3–5]. The remaining questions are the identification of the dominant adsorbed intermediate and the correlated limiting reaction step. To increase the reaction rate, catalyst loadings up to 10 times higher than in PEMFC have been applied [1]. Therefore, much effort is being made to lower the amount [6] and develop new catalysts based on cheaper materials [7–9]. For the anode, a binary catalyst consisting of platinum (Pt) and ruthenium (Ru), often in a 1:1 atomic ratio [7], is most common.

Due to the methanol crossover effect, the situation at the cathode in a DMFC is complex. The cathodic reaction of the PEMFC is well described in the literature [10], but to date, there is no clear understanding of the influence of methanol on the oxygen reduction mechanism [1]. However, the consumption of oxygen due to the methanol oxidation lowers the partial pressure of oxygen, and the formation of a mixed potential at the cathode lowers its potential. A promising approach to avoid this problem is the development of methanol-tolerant catalysts [11]. If this is accomplished, the cathodic overvoltage will be significantly reduced, however,

* Present address: SINTEF Materials and Chemistry, Sem Sælands vei 12, No-7465 Trondheim, Norway. Tel.: +49 761 4588 5213.
E-mail address: anders.oedegaard@ise.fraunhofer.de.

0378-7753/$ – see front matter © 2006 Elsevier B.V. All rights reserved.
doi:10.1016/j.jpowsour.2005.06.030

the utilisation of methanol (or Faraday efficiency) is still low due to the permeation through the membrane.

The best solution to the crossover problem would of course be a new electrolyte which is in-permeable to methanol. DuPont's Nafion®, a perfluorosulfonic acid (PFSA)/polytetrafluorethylene (PTFE) copolymer in the acid form, has been the favoured membrane material for the DMFC for the last 30 years. One way to reduce crossover is to alter its properties, for instance by adding inorganic compounds like silica (SiO_2) [12] and palladium (Pd) [13] or to make physical modifications to the membrane (e.g. grafting [14]) to achieve a barrier against methanol, without limiting the proton transport. New polymer materials, like polybenzimidazole (PBI) and polyphosphazene (PPZ), are also being investigated as alternatives to the sulfonated PFSA [1,15,16]. Despite all these efforts, Nafion® is still the most commonly used membrane material.

In addition to the slow oxygen reduction kinetics, which are strongly influenced by the presence of methanol, the DMFC cathode also exhibits large amounts of water due to the liquid anode feed and the leakage through the membrane. Thus, the danger of flooding is quite substantial. At the same time, the wet environment is also an advantage. A liquid-fed DMFC is not limited to temperatures below 60 °C like a PEMFC if operated without additional humidification. As long as the fuel cell is fed with a liquid methanol–water solution, there is no danger of the membrane drying out. On the other hand, water leaving the cathode has to be recovered and re-injected to the anode feed loop.

A lot of effort has been put into characterising the methanol crossover in DMFC, and the most frequently applied methods involve the measurement of the carbon dioxide (CO_2) content in the cathode outlet by mass spectroscopy (MS), infrared spectroscopy (IR) or gas chromatography (GC) [17–19]. However, the majority of this work is done at elevated temperatures and/or pressures (around 100 °C and up to 3 bar). Generally, the accuracy of all methods is influenced by incomplete cathode oxidation and the presence of intermediate products in the outlet stream, as well as possible CO_2 diffusion from the anode. In measurements presented by Wang et al. [17] and Ren et al. [20], complete conversion of cathodic MeOH to CO_2 is assumed, and a possible CO_2 crossover is not considered. Later investigations have shown contradicting results. Dohle et al. found that the amounts of CO_2 originating from the anode could equal those from methanol crossover at high current densities [21]. Another group claimed that the effect was negligible [22]. The reason for the discrepancies is most probably that the behaviour of the membrane electrode assembly (MEA) is very dependent on the amount of catalyst, the properties of the gas diffusion layer (GDL) and the production/preparation procedure of the MEA.

Dohle et al. found the amount of CO_2 crossover by feeding the cathode with pure nitrogen instead of air. Without oxygen, the crossover methanol cannot oxidise and the measured CO_2 can only originate from the anode. Normal oxidation of methanol and reduction of oxygen take place in the full-cell experiments, see Eqs. (1) and (2). Protons and electrons form hydrogen on the cathode in the half-cell configuration, see Eq. (3), and thus it acts as a reference hydrogen electrode. In practice, electrolysis of methanol takes place. Assuming that the losses at the hydrogen cathode are insignificant, this configuration may also be used to identify the respective electrode overvoltages in a DMFC [23–25].

Anode reaction, full-cell and half-cell:

$$CH_3OH + H_2O \rightarrow CO_2 + 6H^+ + 6e^- \quad (1)$$

Cathode reaction, full-cell:

$$\tfrac{3}{2}O_2 + 6H^+ + 6e^- \rightarrow 3H_2O \quad (2)$$

Cathode reaction, half-cell:

$$6H^+ + 6e^- \rightarrow 3H_2 \quad (3)$$

In contrast to the PEMFC, both the anode and cathode in a DMFC exhibit considerable voltage losses already at relatively low current densities. Several attempts have been made to investigate these electrode effects separately. Due to the constraints of the cell construction and the requirement of physical contact with the electrolyte, it is rather difficult to place a reference electrode in the cell. A dynamic hydrogen electrode (DHE) requires a small applied current between two electrodes positioned on each side of the membrane [26–28]. Ren et al. [28] and Li et al. [29] have evaluated the DHE configuration by comparing it with the half-cell configuration and measured a small deviance in the potentials. At low current densities, the half-cell gave an overvoltage value which was too low, and an overvoltage value which was too high at high current densities. The former was explained by the presence of oxygen in the nitrogen stream and the latter by a noticeable overvoltage due to hydrogen evolution. However, the discrepancies were not large and by using pure hydrogen instead of nitrogen and operating at low current densities, the half-cell operation is a convenient and reliable method to determine the electrode overvoltages.

Impedance spectroscopy has become an increasingly common tool in the characterisation of fuel cells [30]. It is especially useful in systems where the performance is governed by a number of coupled processes proceeding at different rates. For DMFC, though, until recently only a few papers have dealt with such in situ investigations [31]. A major part of the experiments were done at high temperatures and elevated pressures, e.g. [19], but results from single-cell measurements at near-ambient conditions have also been published [24,32–35].

In the literature, there is not much published work on DMFC development and characterisation under ambient conditions. Most of the articles focus on fuel cells operating at elevated temperatures and pressures (around 100 °C and up to 3 bar) and with cell areas exceeding 100 cm^2, e.g. [36–39]. The results obtained are not necessarily transferable to other operating conditions and smaller cells. Therefore, results

from the characterisation of single cells using mass spectroscopy, half-cell operation and impedance spectroscopy under near-ambient conditions, i.e. from room temperature up to 80 °C at 1 atm pressure, are presented in this paper. In addition, single-cell impedance spectra in a previously developed 12-cell stack were also measured, both in full-cell and half-cell operation.

2. Experimental

The experiments were performed using a 5 cm × 5 cm cell with flow-fields milled in 3 mm thick graphite plates. Serpentine flow structures with 1.0 mm wide and deep channels were used at both the anode and the cathode. Nafion® N117 membranes with 1 mg Pt cm^{-2} and 0.5 mg Ru cm^{-2} on the anode and 4 mg Pt cm^{-2} on the cathode were applied as MEA. 270 μm thick graphite paper was used on both sides as GDL. These five-layer MEAs were manufactured by a commercial supplier of fuel-cell components. If not otherwise specified, the cathode was fed with 300 ml min^{-1} air or hydrogen and the anode with 15 ml min^{-1} 1.0 M methanol–water mixture. Polarisation curves were taken at ambient pressure and several temperatures and with varying methanol concentrations. All points were recorded under steady-state conditions, which corresponded to about 5 min per point. During measurement of the polarisation curves, the cathode outlet was connected to a mass spectrometer (MKS minilab, spectra products) to determine the CO_2 content.

A Perkin-Elmer Lock-in Amplifier Model 5210, Princeton Applied Research Potentiostat Model 263A and Kepco Power Booster BOP 20–20 M were used for single-cell impedance spectroscopy experiments. For the simultaneous measurement of single-cell impedances of a stack, a multi-channel impedance analyser, Solartron 1254 Frequency Response Analyser, with two eight-channel extension units Solartron 1251, was applied. The tested 12-cell stack was based on the same type of MEAs as in the single cells and was previously described in [40]. Each impedance measurement was taken at frequencies from 10 kHz down to 100 mHz in 30 steps for the single cells and 40 steps for the stack.

3. Anode and cathode losses

The performance of fuel cells is highly dependent on the operating temperature. Membrane resistance, anode and cathode kinetics as well as mass transport properties are improved by increasing the temperature. Table 1 gives the cell resistance at the different temperatures, and it can be seen that the resistance decreases with temperature. Thus, the membrane is still sufficiently humidified at high temperatures.

In Fig. 1, the IR-corrected total cell and anode overvoltages at operating temperatures from 20 to 80 °C with 1.0 M methanol are shown. The total cell overvoltage is calculated from the experimental polarisation curves and the theoretical open circuit voltage for these conditions, whereas the anode losses are measured in the half-cell. Due to kinetic, ohmic and mass transport effects, the overvoltages increase with current density. A significant decrease in the anode overvoltage is observed with increasing temperature, which can be attributed to improved methanol oxidation. It is considered to be a slow reaction with a strongly adsorbed intermediate. At low temperatures, the total cell overvoltage also decreases with increasing temperatures. However, above 65 °C no further improvement is visible. An identical behaviour was also found for a stack with identical MEAs [41]. Both the electro-osmotic drag and diffusion of methanol and water increase with temperature, which leads to water flooding and mixed potential on the cathode at higher temperatures. Ren et al. reported on the same findings and stated that just before the temperature is high enough to remove cathode water through evaporation in the channels, the danger of flooding is at its maximum [28].

Table 1
Cell resistance at different operating temperatures

Temperature (°C)	Resistance (mΩ cm^{-2})
20	400
35	312.5
50	250
65	242.5
80	237.5

According to the results presented above, the anode accounts for 50–60% of the overall losses at 50 °C. At higher temperatures, the fraction sinks, which is consistent with the literature for DMFC at higher temperatures [23–27] and shows that similar behaviour is valid also at lower temperatures. From 20 to 65 °C, the maximum power density triples from below 20 to almost 60 mW cm^{-2}.

Due to the crossover effect, a varying methanol concentration affects not only the anode. More methanol is transported through the membrane at high MeOH concentrations, so the potential of the cathode decreases and more water is formed. In Fig. 2, the IR-corrected total cell and anode overvoltages with different methanol concentrations at 50 °C are presented. The effect of low concentrations is seen by the limiting currents for operation with 0.10 and 0.25 M. Both electrode overvoltages increase, which is caused by the lack

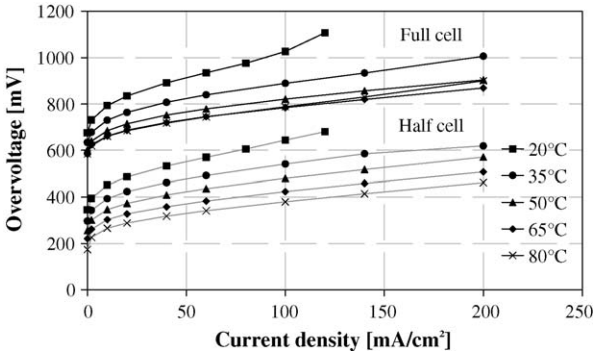

Fig. 1. IR-corrected total cell and anode overvoltages at operating temperatures from 20 to 80 °C with 1.0 M methanol.

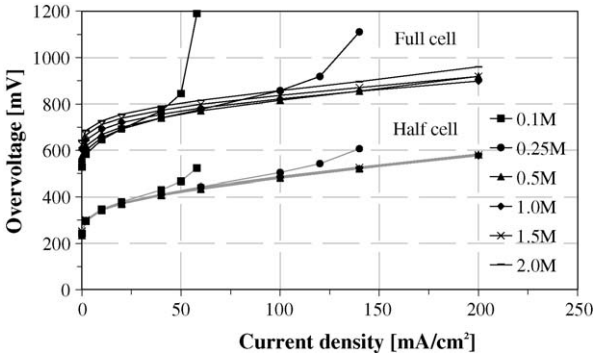

Fig. 2. IR-corrected total cell and anode overvoltages with methanol concentrations from 0.10 to 2.0 M at 50 °C.

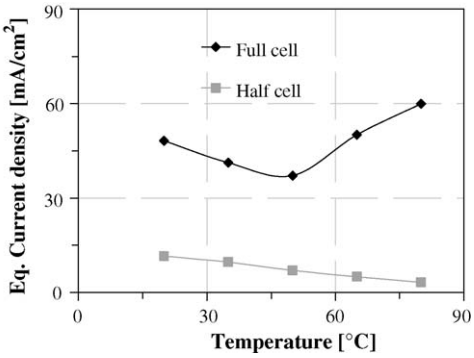

Fig. 3. Equivalent current density of the CO_2 measured in the cathode outlet at different temperatures at 100 mA cm^{-2} and with 1.0 M methanol.

of available methanol and protons at the cathode and anode, respectively. The determined limiting currents correspond to those found by Ren et al. [28].

No changes are visible on the anode overvoltage when the methanol concentration is increased. According to Ren et al., the oxidation rate has a zero-order dependence on methanol in this concentration range [42]. As long as there is a surplus of water in the feed, the methanol kinetics should not be noticeably influenced by the methanol concentration. Similar measurements at higher temperatures also resulted in no change at the anode with the concentration [26,43]. On the other hand, the cathode experiences more methanol and water with increased methanol concentration, which worsens the effect of the already present mixed potential and the danger of water flooding increases. About 60% of the losses can be attributed to the anode, and unlike the effect of the operating temperature, this does not vary much with methanol concentration. The highest cell performance is reached with the 1.0 M methanol solution.

4. CO_2 measurements

During the measurements described above, the cathode outlet was connected to a mass spectrometer and the volumetric ratio of carbon dioxide in the gas flow was determined. Before the experiments started, the mass spectrometer was calibrated with gas mixtures similar to those expected. The full-cell (black line) measurements correspond to both methanol and CO_2 crossover, while the half-cell (grey line) configuration gives only the CO_2 crossover. All data were recorded at 100 mA cm^{-2}.

Fig. 3 shows the equivalent current density of the measured carbon dioxide at different temperatures. Generally, methanol crossover is considered to increase with temperature. For full-cell measurements, a minimum of carbon dioxide in the cathode outlet was found at 50 °C. On the other hand, the half-cell data decrease with temperature, which means that the diffusion of CO_2 through the membrane decreases with temperature. From experiments at constant humidity, it is known that the gas permeability through Nafion® membranes increases with temperature [44]. However, a membrane in contact with liquid water has a higher water uptake at increasing temperatures [45], and a swollen membrane is more gas-tight. This decrease in diffusion of CO_2 through the membrane with temperature, together with the decreasing solubility of CO_2 in water with temperature, can be an explanation for the initial decrease in the amount of CO_2 found in the full-cell cathode outlet in Fig. 3.

Methanol crossover increases also with the anode feed methanol concentration. According to Fig. 4, the full-cell equivalent current density is approximately three times higher with 2.0 M methanol–water mixture than for 0.5 M. A small decrease in CO_2 diffusion is observed (grey line). During water uptake measurements, Ren et al. found that the membrane swelling is proportional to the methanol concentration [28]. The amount of water in the membrane was independent of the MeOH concentration, but methanol uptake increased with concentration. An increased swelling of the membrane can lead to a drop in CO_2 diffusion. At these operating conditions, there are very few comparable data, but Gogel et al. gives a full-cell value somewhat lower than 50 mA cm^{-2} for pressurised operation at 25 °C and with 1.0 M methanol [22].

Fig. 5 shows the equivalent current densities corresponding to the amounts of CO_2 in the cathode outlet throughout a complete polarisation curve. Since the methanol concentration at the anode catalyst-membrane interface decreases with

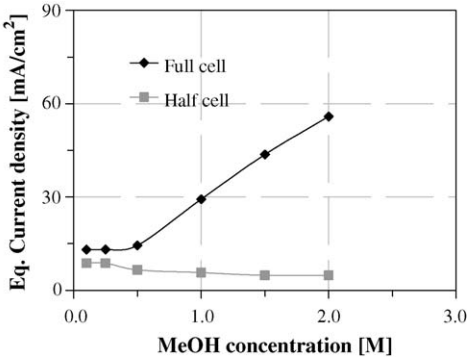

Fig. 4. Equivalent current density of the CO_2 measured in the cathode outlet at different methanol concentrations at 100 mA cm^{-2} and 50 °C.

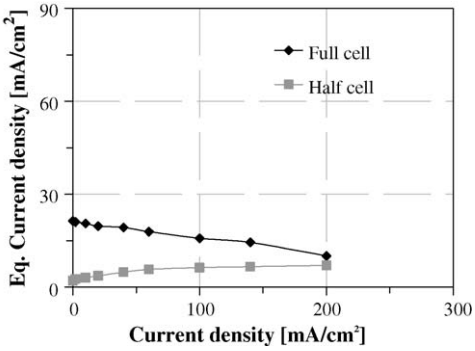

Fig. 5. Equivalent current density of the CO_2 measured in the cathode outlet at different current densities with 0.5 M methanol and at 50 °C.

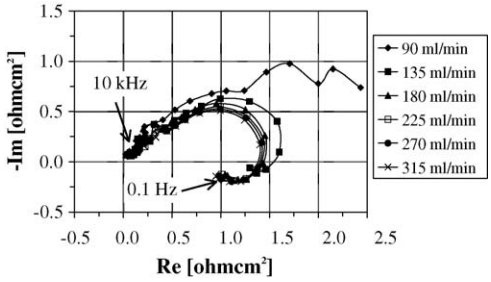

Fig. 7. Nyquist plots of the full-cell impedance at 100 mA cm^{-2} with different air flow rates. Operating conditions: 50 °C, 15 ml min^{-1} 1.0 M methanol and ambient air.

current density, the methanol crossover decreases as well. Thus, the full-cell equivalent current density decreases with the cell current density. By contrast, the half-cell data increase with current density. The quantity of produced CO_2 is proportional to the current, and more carbon dioxide on the anode leads to more diffusion through the membrane. From Fig. 5 it can also be seen that the amount of CO_2 on the cathode at high current densities almost only consists of CO_2 from the anode. These results are obtained at 50 °C and with a 0.5 M methanol solution. At higher methanol concentrations and temperatures, the fraction of methanol crossover will increase considerably, as shown in Figs. 3 and 4. Thereby, the amount of CO_2 from methanol crossover will increase. Dohle et al. measured that approximately 70% of the CO_2 came from the anode at 300 mA cm^{-2}, 85 °C, 1.0 M MeOH and 3 bar [21].

Although it is often assumed that the crossover methanol is immediately converted to carbon dioxide at the cathode [17,20], it is highly unlikely that the conversion is complete. Meier et al. claimed that as much as 20% of the methanol remained [18]. Another group reported methanol concentrations as high as 0.07 M in the liquid cathode outlet (2.0 M MeOH, 90 °C and 100 mA cm^{-2}) [10]. Therefore, to exactly determine the methanol crossover, a catalytic burner is usually included between the cell outlet and the CO_2 analysing equipment [21,22]. In this way, the remaining methanol is completely converted to CO_2. In the experiments presented here, such a procedure was not applied, which may have caused too low values for the crossover to be determined. To estimate the dimension of this error, the methanol concentration in the liquid cathode outlet was determined by external laboratory analysis. Because of the small quantity of liquid at the cathode under these operating conditions, the amount from a whole day of testing was collected and investigated. All cells were operated following the same test procedure, including total duration and current load, so the liquid samples represent an average. The relative values, referred to 50 °C and 1.0 M MeOH, are presented in Fig. 6. At 50 °C and with 1.0 M methanol, the cathode concentration was about 0.01 M, which corresponds to less than 1% of the overall methanol crossover. Thus, it can be said that the MeOH conversion at the cathode was nearly 100%.

The initial increase in methanol concentration with temperature in Fig. 6(a) is caused by the increased crossover. At higher temperatures, a higher conversion rate at the cathode catalyst may lead to the reduction in the amount of methanol. As expected, the amount of non-reacted methanol increases with methanol feed concentration, see Fig. 6(b).

5. Impedance measurements

5.1. Impedance of single cells

With the same cell and experimental set-up as described above, impedance spectra of both full cells and half-cells were measured. Fig. 7 shows the Nyquist plots of the full-cell impedance at 100 mA cm^{-2} with different air flow rates

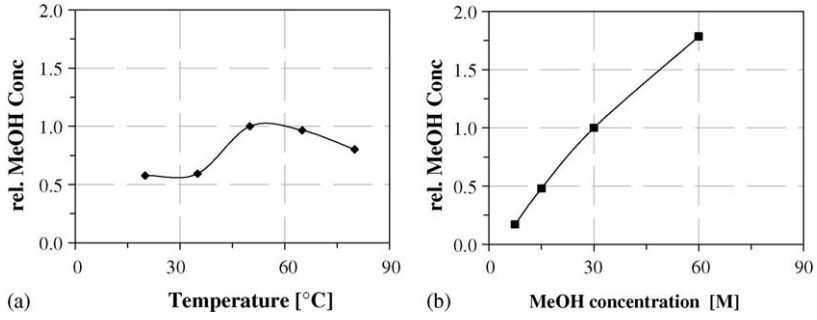

Fig. 6. Relative amounts of methanol in the cathode outlet at different temperatures (a) and methanol concentrations (b), corresponding to the measurements in Figs. 3 and 4, respectively.

at 50 °C. Ninety millilitre per minute corresponds to approximately twice the stoichiometric air flow rate. From the irregular semi-circle at low flow rates, it is immediately seen that the cell experiences a mass transport problem. Due to the dynamic behaviour of the water transport from the cathode (water flooding occurs) and the duration of the impedance measurement at low frequencies, the plot becomes highly irregular. It is not until the flow rate is more than four times higher than the stoichiometric value that further increasing the amount of air does not cause a significant improvement.

Contrary to most hydrogen-fed polymer electrolyte membrane fuel cells, the DMFC also show inductive behaviour. Already in 1968, Schuhmann could explain the inductive part of the Nyquist plot of electrochemical reactions by the adsorption mechanism of intermediates [46]. It is generally accepted that the methanol oxidation is limited by adsorption of carbon monoxide or other intermediates formed. This may also be the reason why inductive behaviour (i.e. positive imaginary impedance) is visible in the low frequency range when mass transport limitations are excluded. Both Müller and Diard have confirmed the inductive part in the DMFC Nyquist plots with kinetic theory, but with a single and triple adsorbate reaction sequence, respectively [31,47]. Another explanation for the inductive behaviour is given by Antoine et al. [48]. They investigated the oxygen reduction reaction on platinum nanoparticles inside Nafion®. This mechanism can also be considered as containing adsorption steps with the adsorbed intermediates, OH_{ads} and O_2H_{ads}. If the cathode reaction is a single step process, these adsorption steps are not included, which lead to the non-inductive behaviour mostly seen in the PEMFC impedance plots [49]. But, in the case of the DMFC cathode, it is possible that this changes in the presence of methanol.

Electrochemical cells, like fuel cells, can be modelled by resistors and capacitors. In a simplified form, a parallel connection of an ohmic resistance and a capacitance represents the electrode–electrolyte interface and a pure ohmic resistance connected in series represents the membrane, see Fig. 8. The electrode ohmic resistance might represent the charge transfer resistance of a reaction, while the capacitance can be attributed to the double-layer capacitance across the interface. A DMFC anode would additionally include an inductance term, as mentioned above. However, the overall situation is much more complicated and physical parameters should be extracted with caution from fitting such models to experimental results. However, the equivalent electric circuit gives a good understanding of the impedance spectra of fuel cells. A model like the one shown in Fig. 8 results in semi-circles, with the size and position depending on the value of the resistances and capacitances. The measured Nyquist plots, such as those shown in Fig. 7, are more flattened semi-circles. This is caused by the inhomogeneous spatial distribution of mass, temperature and current in the cell [30] and the roughness of the dispersed electrode surfaces [50]. An overlap between different semi-circles is also possible if the effects are activated in the same frequency regions. If the cathode is fed with hydrogen, only the anode resistance and capacitance and the membrane resistance will show in the impedance spectra.

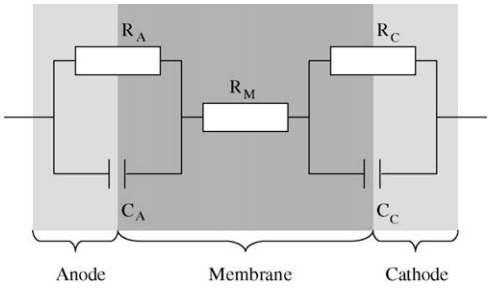

Fig. 8. Equivalent electric circuit describing a fuel cell, after [30,31].

The methanol flow rate is not as critical for the performance as the air flow rate. Basically, removal of CO_2 gas bubbles with a liquid is much easier than removal of water droplets with gas. The stoichiometric flow rate of 1.0 M methanol at 100 mA cm^{-2} is about 0.25 ml min^{-1}. However, the parasitic methanol loss due to crossover is also significant, and amounts of up to 100% of the useful MeOH consumption have been reported [22,42]. Thus, the real stoichiometric flow rate is up to two times higher. Nyquist plots of the full-cell and half-cell impedance at 100 mA cm^{-2} with different methanol flow rates are shown in Fig. 9(a) and (b). In the full-cell plot (a), the curves represent both the anode and cathode impedance. Here, a local maximum is seen at high frequencies, which can be attributed to the cathode reduction. The second semi-circle corresponds to the anode processes and resembles the semi-circle for half-cell operation. A methanol flow rate, which is too low, also influences the cathode. This is evident since the full-cell impedance at 0.5 ml min^{-1} is much

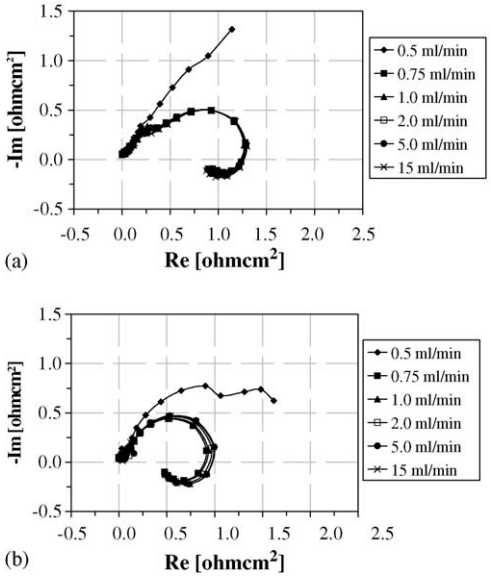

Fig. 9. Nyquist plots of the full-cell (a) and half-cell (b) impedance at 100 mA cm^{-2} with different methanol flow rates. Operating conditions: 50 °C, 1.0 M methanol and 300 ml min^{-1} air or hydrogen at ambient conditions.

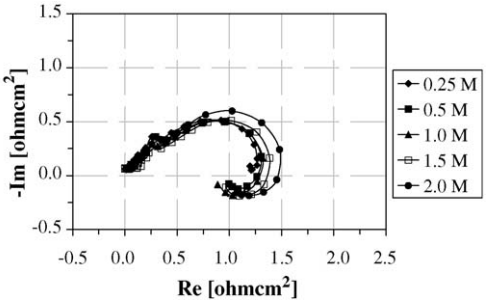

Fig. 10. Nyquist plots of the full-cell impedance at 100 mA cm^{-2} with different methanol concentrations. Operating conditions: 50 °C, 15 ml min^{-1} methanol and 300 ml min^{-1} air at ambient conditions.

higher than the half-cell impedance. The reduction of oxygen may be limited by the transport of protons and electrons to the cathode. If both the oxidised and crossover methanol is considered, a methanol flow rate of less than two times the real stoichiometric flow rate is sufficient for stable operation. A further increase of the flow rate has no significant effect.

In Fig. 10, the Nyquist plots of the full-cell impedance at different methanol concentrations are shown. Here, the 45° slope of the curves at high frequencies is more pronounced than in the previous graphs. Generally, this is known from electrochemical cells with porous electrodes and limited electrolyte conductivity, and can be related to the coupling of the distributed ionic resistance and the distributed capacitance in the catalyst layer [49,51]. The influence of methanol concentration on the performance was also shown in the polarisation curves in Fig. 2. Since the effect of methanol concentration on the anode is minimal, both of these results show that the cathode losses increase with methanol concentration. Additionally, the impedance measurements reveal an increased inductive behaviour with concentration. The same behaviour was also seen in the anode Nyquist plots. If more water is available at the catalyst, the oxidation of the adsorbed intermediate is faster. This is valid for both the anode and the cathode. Other differences in the anode Nyquist plots with methanol concentration were not observed.

From the measurements presented in Fig. 1, it was assumed that only the anode kinetics improve with temperature. When the Nyquist plots of the full-cell impedance in Fig. 11(a) are examined, a decrease of the local maximum at high frequencies with temperature is noticed. This may indicate that the oxygen reduction in DMFC also improves with temperature. However, this could not be seen in the polarisation curves in Fig. 1. The methanol and water crossover also increases with temperature, and the strong effect of the methanol-air mixed potential and water flooding at the cathode suppress the temperature dependence of the electrode kinetics in the polarisation curve. Just as in Fig. 1, the anode losses in Fig. 11(b) decrease with temperature. The oxidation of methanol, including intermediates, is faster at elevated temperatures. Therefore, the inductive part corresponding to the poisoning adsorption step is also smaller.

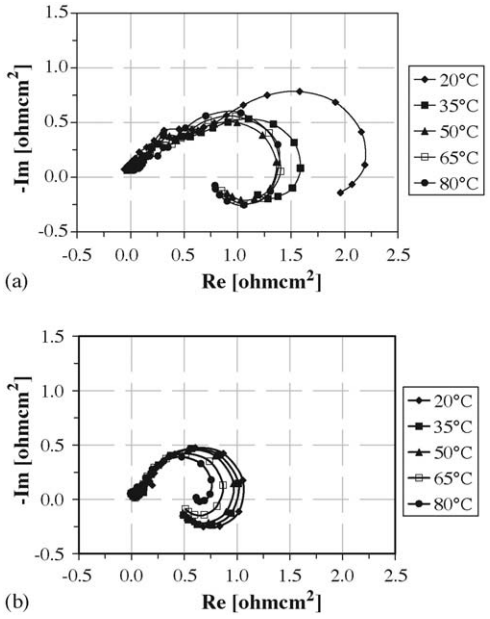

Fig. 11. Nyquist plots of the full-cell (a) and half-cell (b) impedance at 100 mA cm^{-2} and different operating temperatures. Operating conditions: 15 ml min^{-1} 1.0 M methanol and 300 ml min^{-1} air or hydrogen at ambient conditions.

As long as no mass transport problems occur, the cathode accounts for approximately one third of the total losses. At low temperatures, the anode kinetics are limiting, whereas at higher temperatures the mass transport at the cathode (water) is limiting. This agrees with the conclusions in [19,24,52].

5.2. Impedance stack

It has already been shown that the performance of direct methanol fuel cells strongly depends on the operating conditions, e.g. air and methanol flow rates, operating temperature and methanol concentration. Although there are small temperature and concentration gradients in a stack, the inhomogeneous delivery of reactants to and removal of products from the cells mostly cause the unstable and non-uniform behaviour of the single-cell voltages [41]. Already at low current densities, there is a difference of several millivolt between the best and the worst cell. This difference increases continuously, until one or more single-cell voltages rapidly drop as the current is raised. When the current is increased even more, several cell voltages start to oscillate and eventually drop to negative values. Fig. 12 shows the Nyquist plots of the full-cell impedance for all 12 cells simultaneously in a stack at 70 mA cm^{-2}.

These Nyquist plots have the same typical character of a DMFC as those of single cells, with the 45° slope at high frequencies and the inductive part at low frequencies, see Fig. 10. The majority of the cells show almost identical plots, but in cells 2, 3 and 4, a second semi-circle is visible. Usually, this is interpreted as being due to mass transportation problems. However, from Fig. 12 it is difficult to see exactly

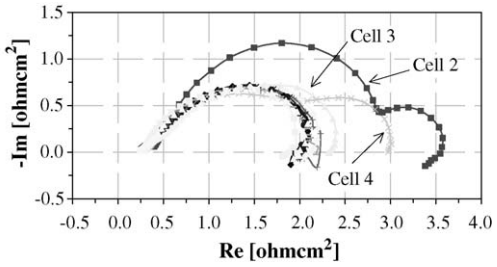

Fig. 12. Nyquist plots of the full-cell impedance for all 12 cells at 70 mA cm^{-2}. Operating conditions: 50 °C, 60 ml min^{-1} 1.0 M methanol and 4.7 l min^{-1} ambient air.

where or what the limiting effect can be. By applying the same half-cell measurement configuration as described previously to the stack, the anode and cathode impedance can be separated. Fig. 13 presents the Nyquist plots of the half-cell (anode) impedance under the same conditions as for the plots in Fig. 12.

Since the applied MEAs are identical to those in the single-cell experiments, these anode impedance plots are essentially the same as those presented before, see also Fig. 11(b). Differences are mainly due to different current densities in the two measurements. The deviation between the 12 Nyquist plots is very small, which indicates that the conditions at the anodes are practically equal. Alternatively, the possible differences have no influence on the anode impedance plot and the performance. In Fig. 14, however, where the cathode Nyquist plots are depicted, a serious discrepancy between the impedance curves is found. The increased size of the cathode curves indicates that mass transport limitation occurs. Water flooding of some electrodes leads to a decreased active area in those cells, and thus, an increased ohmic resistance and cathode impedance evolve. Removal of the cathode water is dependent on homogeneous air distribution to all cells by the manifolds.

An inductive behaviour is also observed at the cathode, which probably relates to the oxidation of crossover-methanol. In the cells where no mass transport limitation occurs, the low frequency part of the cathode impedance is

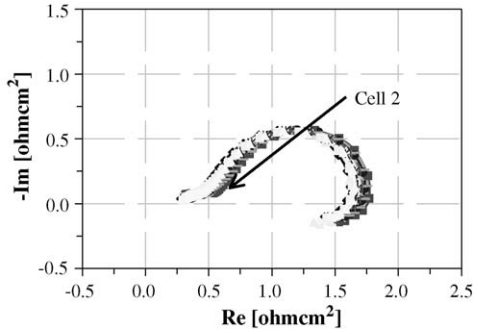

Fig. 13. Nyquist plots of the half-cell impedance for all 12 cells at 70 mA cm^{-2}. Operating conditions: 50 °C, 60 ml min^{-1} 1.0 M methanol and 4.7 l min^{-1} hydrogen.

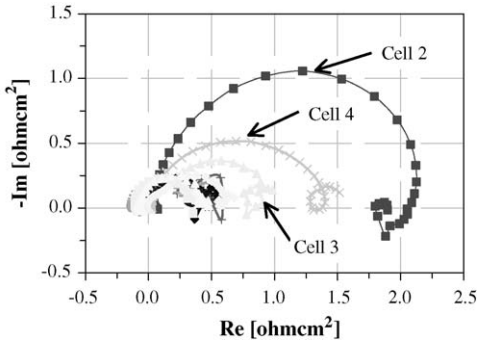

Fig. 14. Calculated cathode Nyquist plots based on the results in Figs. 12 and 13.

about 1/3 of the total, see Figs. 12 and 14, the same relationship as obtained previously with single cells.

6. Conclusion

A thorough characterisation of direct methanol fuel cells under ambient conditions has been presented. At varying operating temperature and methanol concentration, full-cell and half-cell overvoltages were examined by feeding the cathode with hydrogen and using it as a reference electrode. The dependence of these overvoltages on temperature and concentration were further compared with impedance spectroscopy experiments. Both the anode and the cathode kinetics improve with increasing temperature, but the cathode suffers from losses due to higher methanol crossover and water flooding at higher temperatures. The methanol concentration, however, mainly influences the cathode. Measurements of CO_2 in the cathode outlet revealed that the amount of crossover CO_2 is noticeable compared to the CO_2 from methanol crossover, but decreases with temperature and methanol concentration. Almost 100% of the crossover methanol is converted to CO_2 at the cathode. With a multi-channel impedance spectrometer, the single-cell impedance spectra of all cells in a stack were measured simultaneously. It could be seen that the cathodes limit the stack performance due to water flooding and methanol crossover.

Acknowledgements

The author would like to thank Jan Clausnitzer for performing the stack impedance measurements and Alexander Hakenjos for lending the multi-channel impedance test station.

References

[1] R. Dillon, S. Srinivasan, A.S. Aricò, V. Antonucci, J. Power Sources 127 (2004) 112–126.
[2] P. Costamagna, S. Srinivasan, J. Power Sources 102 (2001) 242–252.

[3] S. Wasmus, A. Küver, J. Electroanal. Chem. 461 (1999) 14–31.
[4] A. Hamnett, Catal. Today 38 (1997) 445–457.
[5] M.P. Hogarth, T.R. Ralph, Platinum Met. Rev. 46 (49) (2002) 146–164.
[6] A.S. Aricò, V. Baglio, E. Modica, A. Di Blasi, V. Antonucci, Electrochem. Commun. 6 (2004) 164–169.
[7] E. Antolini, Mater. Chem. Phys. 78 (2003) 563–573.
[8] Z. Wei, S. Wang, B. Yi, J. Liu, L. Chen, W.J. Zhou, W. Li, Q. Xin, J. Power Sources 106 (2002) 364–369.
[9] W.C. Choi, J.D. Kim, S.I. Woo, Catal. Today 74 (2002) 235–240.
[10] A. Hamnett, Handbook of Fuel Cells, vol.1, John Wiley & Sons Ltd, Chichester, United Kingdom, 2003 (Chapter 18).
[11] R.W. Reeve, P.A. Christensen, A.J. Dickinson, A. Hamnett, K. Scott, Electrochim. Acta 45 (2000) 4237–4250.
[12] P.L. Antonucci, A.S. Aricó, P. Creti, E. Ramunni, V. Antonucci, Solid State Ionics 125 (1999) 431–437.
[13] W.C. Choi, J.D. Kim, S.I. Woo, J. Power Sources 96 (2001) 411–414.
[14] K. Scott, W.M. Taama, P. Argyropoulos, J. Membr. Sci. 171 (2000) 119–130.
[15] A. Heinzel, V.M. Barragán, J. Power Sources 84 (1999) 70–74.
[16] J.A. Kerres, J. Membr. Sci. 185 (2001) 3–27.
[17] J.-T. Wang, S. Wasmus, R.F. Savinell, J. Electrochem. Soc. 143 (4) (1996) 1233–1239.
[18] F. Meier, S. Denz, A. Weller, G. Eigenberger, Fuel Cells 3 (4) (2003) 161–168.
[19] J.T. Müller, Ph.D. thesis, Shaker Verlag, Aachen, Germany, 2000.
[20] X. Ren, W. Henderson, S. Gottesfeld, J. Electrochem. Soc. 144 (9) (1997) L267–L270.
[21] H. Dohle, J. Divisek, J. Mergel, H.F. Oetjen, C. Zingler, D. Stolten, J. Power Sources 105 (2002) 274–282.
[22] V. Gogel, T. Frey, Z. Yongsheng, K.A. Friedrich, L. Jörissen, J. Garche, J. Power Sources 127 (2004) 172–180.
[23] B. Gurau, A. Smotkin, J. Power Sources 112 (2002) 339–352.
[24] J.C. Amphlett, B.A. Peppley, E. Halliop, A. Sadiq, J. Power Sources 96 (2001) 204–213.
[25] K. Scott, A.K. Shukla, C.L. Jackson, W.R.A. Meuleman, J. Power Sources 126 (1–2) (2004) 67–75.
[26] A. Küver, I. Vogel, W. Vielstich, J. Power Sources 52 (1994) 77–80.
[27] M.K. Ravikumar, A.K. Shukla, J. Electrochem. Soc. 143 (8) (1996) 2601–2606.
[28] X. Ren, T.E.X. Springer, S. Gottesfeld, J. Electrochem. Soc. 147 (1) (1997) 92–98.
[29] G. Li, P.G. Pickup, Electrochim. Acta 49 (2004) 4119–4126.
[30] E. Ivers-Tiffée, A. Weber, H. Schichlein, Handbook of Fuel Cells, vol. 2, John Wiley & Sons Ltd, Chichester, United Kingdom, 2003 (Chapter 17).
[31] J-P. Diard, N. Glandut, P. Landaud, B. Le Gorrec, C. Montella, Electrochim. Acta 48 (2003) 555–562.
[32] N. Nakagawa, Y. Xiu, J. Power Sources 118 (2003) 248–255.
[33] J. Otomo, Y. Kondo, C. Wen, K. Eguchi, K. Yamada, H. Takahashi, J. School Eng. XLVII (2000) 29–42.
[34] K. Richau, V. Kudela, J. Schauer, R. Mohr, Macromol. Symp. 188 (2002) 73–89.
[35] Y.-C. Liu, X.-P. Qiu, W.-T. Zhu, G.-S. Wu, J. Power Sources 114 (2003) 10–14.
[36] P. Argyropoulos, K. Scott, W.M. Taama, Chem. Eng. J. 73 (1999) 217–227.
[37] D. Buttin, M. Dupont, M. Straumann, R. Gille, J.-C. Dubois, R. Ornelas, G.P. Fleba, E. Ramunni, V. Antonucci, A.S. Aricó, P. Creti, E. Modica, J. Appl. Electrochem. 31 (2001) 275–279.
[38] H. Dohle, H. Schmitz, T. Bewer, J. Mergel, D. Stolten, J. Power Sources 106 (2002) 313–322.
[39] A.K. Shukla, M.K. Ravikumar, M. Neergat, K.S. Gandhi, J. Appl. Electrochem. 29 (1999) 129–132.
[40] A. Oedegaard, S. Hufschmidt, R. Wilmshoefer, C. Hebling, Fuel Cells 4 (3) (2004) 219–224.
[41] A. Oedegaard, J. Power Sources, in press, doi:10.1016/j.powsour.2005.06.044.
[42] X. Ren, S.C. Thomas, P. Zelenay, S. Gottesfeld, J. Power Sources 86 (2000) 111–116.
[43] A. Küver, W. Vielstich, J. Power Sources 74 (1998) 211–218.
[44] P. Gode, G. Lindbergh, G. Sundholm, J. Electroanal. Chem. 518 (2002) 115–122.
[45] J. Shim, H.Y. Ha, S.-A. Hong, I.-H. Oh, J. Power Sources 109 (2002) 412–417.
[46] D. Schumann, J. Electroanal. Chem. 17 (1968) 45–59.
[47] J.T. Müller, P.M. Urban, W.F. Hölderich, J. Power Sources 84 (1999) 157–160.
[48] O. Antonie, Y. Bultel, R. Durand, J. Electroanal. Chem. 499 (2001) 85–94.
[49] D. Gerteisen, A. Hakenjos, J. Schumacher, J. Electrochem. Soc., submitted for publication.
[50] J.T. Müller, P.M. Urban, J. Power Sources 75 (1998) 139–143.
[51] B. Andreaus, G.G. Scherer, Proceedings of the Second European Fuel Cell Forum, vol. 1, Lucerne, Switzerland, 2003, pp. 373–382.
[52] A. Siebke, Ph.D. thesis, VDI Verlag GmbH, Düsseldorf, Germany, 2003.